

Functional significance of the two ACOX1 isoforms and their crosstalks with PPAR α and RXR α

Aurore Vluggens^{1,2,3}, Pierre Andreoletti^{1,2}, Navin Viswakarma³, Yuzhi Jia³, Kojiro Matsumoto³, Wim Kulik⁴, Mushfiquddin Khan⁵, Jiansheng Huang³, Dongsheng Guo³, Sangtao Yu³, Joy Sarkar³, Inderjit Singh⁵, M Sambasiva Rao³, Ronald J Wanders⁴, Janardan K Reddy³ and Mustapha Cherkaoui-Malki^{1,2}

Disruption of the peroxisomal acyl-CoA oxidase 1 (*Acox1*) gene in the mouse results in the development of severe microvesicular hepatic steatosis and sustained activation of peroxisome proliferator-activated receptor- α (PPAR α). These mice manifest spontaneous massive peroxisome proliferation in regenerating hepatocytes and eventually develop hepatocellular carcinomas. Human ACOX1, the first and rate-limiting enzyme of the peroxisomal β -oxidation pathway, has two isoforms including ACOX1a and ACOX1b, transcribed from a single gene. As ACOX1a shows reduced activity toward palmitoyl-CoA as compared with ACOX1b, we used adenovirally driven ACOX1a and ACOX1b to investigate their efficacy in the reversal of hepatic phenotype in *Acox1*($-/-$) mice. In this study, we show that human ACOX1b is markedly effective in reversing the ACOX1 null phenotype in the mouse. In addition, expression of human ACOX1b was found to restore the production of nervonic (24:1) acid and had a negative impact on the recruitment of coactivators to the PPAR α -response unit, which suggests that nervonic acid might well be an endogenous PPAR α antagonist, with nervonoyl-CoA probably being the active form of nervonic acid. In contrast, restoration of docosahexaenoic (22:6) acid level, a retinoid-X-receptor (RXR α) agonist, was dependent on the concomitant hepatic expression of both ACOX1a and ACOX1b isoforms. This is accompanied by a specific recruitment of RXR α and coactivators to the PPAR α -response unit. The human ACOX1b isoform is more effective than the ACOX1a isoform in reversing the *Acox1* null phenotype in the mouse. Substrate utilization differences between the two ACOX1 isoforms may explain the reason why ACOX1b is more effective in metabolizing PPAR α ligands.

Laboratory Investigation (2010) 90, 696–708; doi:10.1038/labinvest.2010.46; published online 1 March 2010

KEYWORDS: fatty acids oxidation; hepatic steatosis; peroxisome proliferation; PPAR α ; RXR α

Mice lacking acyl-CoA oxidase 1 (*Acox1*), which catalyzes the first and rate-limiting enzyme of the peroxisomal fatty acid β -oxidation pathway of very-long-chain fatty acids (VLCFAs), develop severe microvesicular steatohepatitis with increased intrahepatic H₂O₂ levels and hepatocellular regeneration.^{1,2} Liver cell proliferation leads to complete replacement of steatotic hepatocytes with hepatocytes that exhibit massive spontaneous peroxisome proliferation.¹ Older *Acox1*($-/-$) mice develop hepatocellular carcinomas due to the sustained activation of peroxisome proliferator-activated receptor- α (PPAR α).² Mice nullizygous for both *Ppar α* and *Acox1* (*Ppar α* ($-/-$), *Acox1*($-/-$)), have shown a lack of spontaneous hepatic peroxisome proliferation and

a marked decrease in hepatic steatosis, which emphasizes the critical role of both PPAR α and ACOX1 in hepatic metabolism and in the pathogenesis of specific fatty liver phenotype.³ Sustained activation of PPAR α and transcriptional activation of PPAR α target genes in the liver of mice lacking ACOX1 highlight the role of peroxisomal ACOX1 in metabolizing the endogenous natural PPAR α ligands.⁴

At the transcriptional level, PPAR α , which forms a heterodimer with retinoid X receptor (RXR),^{5,6} binds to peroxisome proliferator-responsive element (PPRE) present in the 5'-flanking region of target genes.^{6–8} In the presence of a ligand, PPAR–RXR complexes recruit coactivators, such as steroid receptor coactivator-1 (SRC-1) and PPAR-binding

¹INSERM, UMR 866, Dijon, France; ²Centre de Recherche-Biochimie Métabolique et Nutritionnelle (LBMN), Université de Bourgogne, GDR CNRS 2583, Dijon, France; ³The Department of Pathology, Northwestern University, Feinberg School of Medicine, Chicago, IL, USA; ⁴Laboratory Genetic Metabolic Diseases, Department of Clinical Chemistry and Pediatrics, Emma Children's Hospital, Academic Medical Center, University of Amsterdam, Meibergdreef 9, Amsterdam, The Netherlands and ⁵Department of Pediatrics, Charles Darby Children's Research Institute, Medical University of South Carolina, Charleston, SC, USA
Correspondence: Professor M Cherkaoui-Malki, PhD, Centre de Recherche INSERM, U866, LBMN, Université de Bourgogne, 6, Boulevard Gabriel, Dijon 21000, France. E-mail: malki@u-bourgogne.fr

Received 23 June 2009; revised 22 December 2009; accepted 22 December 2009

protein/Mediator 1 (PBP/TRAP220/Med1)^{9,10} to enhance target gene transcription.^{9–11} The generation of *Ppar α* ^{-/-} mice established that PPAR α is essential for hepatic peroxisome proliferation and coordinates transcriptional activation of genes coding for ACOX1, L-peroxisomal bifunctional enzyme (L-PBE), peroxisomal thiolase (PTL), cytochrome P₄₅₀4A10 (CYP4A10) and cytochrome P₄₅₀4A14 (CYP4A14), and other lipid metabolism-related key enzymes by structurally diverse synthetic peroxisome proliferators, as well as by several fatty acids and their polyunsaturated derivatives.^{12–15}

Although fatty acids are metabolized by the mitochondrial and peroxisomal β -oxidation enzyme systems with partly overlapping substrate specificities,^{3,16} the oxidation of the major fraction of medium and long-chain fatty acids (LCFAs, C12–C18) occurs in the mitochondria, whereas oxidation of VLCFAs takes place almost exclusively in peroxisomes.^{3,16} Both LCFAs and VLCFAs (>C18) are also metabolized by the microsomal CYP4A10 and CYP4A14 fatty acid ω -hydroxylases, resulting in the formation of dicarboxylic acids (DCAs) that are further degraded by the peroxisomal β -oxidation system.^{16,17}

In several peroxisomal disorders, the peroxisomal fatty acid β -oxidation pathway is defective either with a decreased number or the absence of morphologically distinguishable peroxisomes in the liver. One of these peroxisomal disorders is pseudoneonatal adrenoleukodystrophy (P-NALD), caused by ACOX1 deficiency.¹⁸ The ACOX1 enzyme is encoded by a single gene, which generates two splice variants, including exon 3a or exon 3b, respectively,^{19,20} leading to the synthesis of two protein isoforms ACOX1a or ACOX1b.²¹ A single homozygous mutation in exon 3b results in the development of the P-NALD disease,²² suggesting different substrate specificities of the two ACOX1 isoforms. On the other hand, further biochemical analysis of recombinant human ACOX1 isoforms showed that ACOX1a seems to be more labile and exhibits only 50% specific activity toward palmitoyl-CoA as compared with ACOX1b.²¹

Therefore, in an attempt to approach the *in vivo* conditions and to understand the sensing metabolic role of ACOX1 *vis-à-vis* the hepatic steatosis and the activation of PPAR α , we expressed human ACOX1 isoforms in *Acox1*(^{-/-}) null mice by adenofection. We then analyzed the impact of human ACOX1 expression on the pathophysiological aspects and on the regulation of PPAR α and its target genes in the liver samples obtained from *Acox1*(^{-/-}) mice. We now show that the hepatic expression of human ACOX1b isoform reverses the phenotype of *Acox1*(^{-/-}) null mice.

MATERIALS AND METHODS

Adenoviral Gene Transfer

Construction of recombinant adenovirus containing the human ACOX1a or ACOX1b cDNA (Ad/hACOX1a or Ad/hACOX1b) was as follows. Human ACOX1a or ACOX1b cDNAs²¹ were cloned into the BglIII and HindIII sites of pShuttle-CMV expression vector (Quantum Biotechnologies).

A nucleotide sequence encoding 6xHis-tag was introduced into the 5'-flanking regions of each cDNA between BglIII/KpnI sites. The linearized pShuttle vector and AdEasy vector (Quantum Biotechnologies) were then cotransformed into the *Escherichia coli* strain BJ5183. Positive recombinant plasmid Ad/hACOX1a or Ad/hACOX1b were selected. The Ad/hACOX1a or Ad/hACOX1b virus was then generated as described previously.²³ The adenoviral construct of Ad/LacZ was a generous gift from Dr W El-Deiry (University of Pennsylvania, Philadelphia, PA, USA) and has been described previously.²³

Mice and Treatments

Both wild-type (C57BL/6J) and *Acox1*^{-/-} mice,^{1,2} 6–10 weeks of age, were used in this study. Mice were kept under a 12-h light/12-h dark cycle, and maintained on powdered chow and water *ad libitum*. Recombinant adenovirus Ad/hACOX1a, Ad/hACOX1b or Ad/lacZ were injected intravenously through the tail vein, in a volume of 200 μ l with 2×10^{11} virus particles and killed 5 days after injection. For cell proliferation analysis, mice were administered bromodeoxyuridine (BrdUrd) (1 mg/ml) in drinking water for 3 days after adenovirus injection, and their livers were processed for immunohistochemistry.²³ The animal procedures used in this study were approved by the Institutional Review Boards for Animal Research of the Northwestern University.

RESULTS

ACOX1: One Gene, Two Splice Variants with Differential Tissue Expressions

In both humans and mouse, the *ACOX1* gene consists of 15 exons and 14 introns, with exon 3 presenting as two variants 3a and 3b, respectively, leading to the synthesis of an ACOX1a and ACOX1b isoform.^{19–21} Indeed, alternative splicing of pre-mRNA produces two mRNA sequences harboring exon 3a or exon 3b, which both code for a 54 amino-acid region located near the N terminus. This region is highly conserved in several species with high amino-acid identity.^{19,20} Alignment of amino-acid sequences from humans (hEx3a and hEx3b) and mouse (mEx3a and mEx3b) shows 87% identity between hACOX1a and mACOX1a, and 94% identity between hACOX1b and mACOX1b (Supplementary Figure S1A). This strong conservation through evolution suggests that the two isoforms may well have different physiological functions. In human tissues, both the a and the b isoforms show essentially similar levels of expression (Supplementary Figure S1B). In the mouse, the *Acox1b* mRNA level appeared higher in white adipose tissue (Supplementary Figure S1B). Higher level of expression of 1a over 1b in the liver and kidney or inversely 1b over 1a in the brain, lung, muscle, white adipose tissue and testis are evident. In the human heart, both splice variants are expressed equally (Supplementary Figure S1B). This differential expression shows the existence of a tissue-dependent splice regulation of *Acox1* mRNAs.

Table 1 Acyl-CoA oxidase activities in liver homogenates of wild-type (Wt) and *Acox1* null mice (*-/-*) expressing β -galactosidase protein (*-/-* LacZ) or human ACOX1 isoforms (*-/-* 1a, *-/-* 1b or *-/-* 1ab)

Genotype	ACOX1 activity (pmols/min per mg)
Wt	101 \pm 6.74
<i>-/-</i>	0
<i>-/-</i> LacZ	0
<i>-/-</i> 1a	3 \pm 0.89
<i>-/-</i> 1b	27 \pm 13
<i>-/-</i> 1ab	23 \pm 8.9

Values are means \pm s.d.

General Approach

The availability of *Acox1*(*-/-*) mice enabled us to determine the immediate effects of transient expression of human ACOX1 isoforms a and b²¹ on PPAR α -mediated pleiotropic responses in mouse hepatocytes *in vivo*. *Acox1*(*-/-*) mice develop severe microvesicular steatohepatitis, which leads to progressive hepatocellular regeneration. The regenerated hepatocytes exhibit massive spontaneous peroxisome proliferation accompanied by a sustained activation of PPAR α and its target genes.¹⁻³ The expression of human ACOX1 isoforms by adenofection in the *Acox1*(*-/-*) mouse liver was attested by real-time quantitative PCR at the mRNA level and by western blotting and measurement of enzymatic activity toward palmitoyl-CoA (Table 1 and Supplementary Figure S2). Results obtained from time-course experiments (3, 5 and 7 days) show that the expression level of ACOX1a or ACOX1b reaches a maximum at 5 days after infection and declines abruptly at 7 days (Supplementary Figures S3 and S4). Despite a higher adenofection dose, it was not possible to express ACOX1a to a similar extent as ACOX1b in *Acox1*(*-/-*) mouse liver (Supplementary Figure S5). However, additional analyses using real-time PCR and immunostaining methods show an evident expression of ACOX1a at both mRNA and protein levels. However, when compared with the activity level of ACOX1b, ACOX1a expression was 10-fold lower (Table 1 and Supplementary Figures S3-S5).

Influence of Human ACOX1 Isoform Expression on Hepatic Steatosis in ACOX1 Null Mouse

The absence of ACOX1 in the liver of ACOX1 null mice caused microvesicular fatty metamorphosis of hepatocytes (Figure 1a). Fatty changes were detected in all hepatocytes irrespective of their distribution within the liver lobule, but were not found in regenerated liver cells after their emergence. These showed abundant intensely eosinophilic granular cytoplasm (Figure 1a). The expression of the ACOX1a isoform in the *Acox1*(*-/-*) mouse liver (Figure 1a) resulted in a modest reduction in hepatic steatosis as compared with

Acox1(*-/-*) livers. On the other hand, the expression of ACOX1b resulted in a significant reduction in hepatic steatosis (Figure 1a and *-/-*1b insert). The expression of ACOX1b was robust in many hepatocytes as concluded from the intense cytoplasmic peroxidase staining, whereas in other hepatocytes, the expression was less pronounced (Figure 1b and *-/-*1b insert). The concomitant expressions of both ACOX1a and ACOX1b isoforms show a near complete reversal of fatty liver phenotype in *Acox1*(*-/-*) (Figure 1b and *-/-*1b insert). In addition, when the expression level of ACOX1a isoform is enhanced twice in the *Acox1*(*-/-*) liver, we observed only a weak reversal of the hepatic steatosis phenotype in these mice (Supplementary Figure S5).

Hepatic Lipid Storage and Serum Fatty Acid Profiles

Human ACOX1a expression in the *Acox1* null mouse liver resulted in a mild reduction in neutral lipid content and this correlated with an appreciable reduction in microvesicular steatosis in hepatocytes (Figure 2). The expression of ACOX1b resulted in a marked decrease in the neutral lipid oil-red O staining when compared with *Acox1*(*-/-*) null mice (Figure 2, Wt and *-/-*1b inserts). The expression of both isoforms 1a and 1b in the *Acox1*(*-/-*) liver essentially reversed hepatic steatosis with a staining lipid profile resembling the wild-type phenotype (Figure 2, Wt and *-/-*1ab inserts).

In ACOX1 null mice, the absence of peroxisomal fatty acid oxidation resulted in a decrease in circulating triacylglycerol (TG) level (Supplementary Figure S3C). The expression of each ACOX1 isoform shows a significant increase in serum TG at 3 days for ACOX1a and at both 3 and 5 days for ACOX1b (Supplementary Figure S3 and S4). The expression of both human isoforms 1a and 1b in *Acox1*(*-/-*) mice is accompanied by a strong hypertriglyceridemia (Supplementary Figure S5). Plasma cholesterol level shows a significant increase only when both ACOX1 isoforms are coexpressed in the *Acox1*(*-/-*) liver (Supplementary Figure S5).

ACOX1B Controls the Spontaneous Hepatic Peroxisome Proliferation

Visualization of semithin sections of the liver of 2-month-old *Acox1*(*-/-*) mice, showed a paucity of peroxisomes in the majority of hepatocytes that exhibit microvesicular lipid droplets. In these cells, the diaminobenzidine-positive catalase-containing organelles were sparse (Figure 3 and *-/-* lower left insert). As reported previously, *Acox1*(*-/-*) livers showed progressive cell proliferation, and the newly emerging hepatocytes show spontaneous peroxisome proliferation (Figure 3 and *-/-* lower right insert). *Acox1*(*-/-*) livers, in which the ACOX1a isoform was expressed, exhibited many fatty hepatocytes but with smaller lipid droplets (Figure 3 and *-/-*1a upper right insert) when compared with the larger fat droplets in the *Acox1*(*-/-*) liver (Figure 3 and *-/-* lower left insert). In the liver of the *Acox1* null mice, expressing the ACOX1b isoform, the majority of hepatocytes

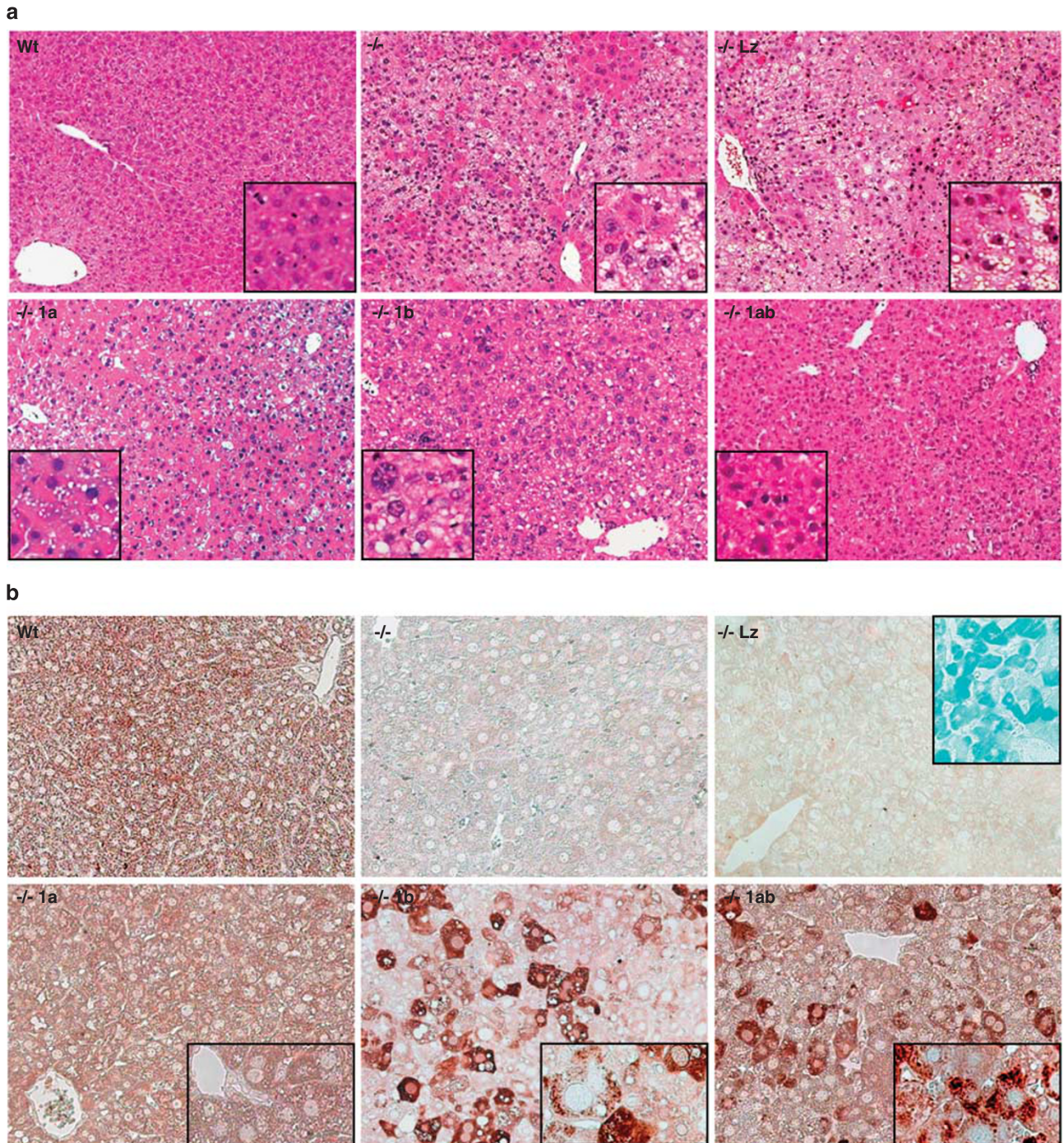


Figure 1 Hepatic steatosis attenuation after adenovirus-hACOX1a and hACOX1b expression in *Acox1*^{-/-} mice. *Acox1*^{-/-} mice were injected with recombinant adenovirus: Ad/hACOX1a, Ad/hACOX1b or both Ad/hACOX1a and Ad/hACOX1b particles intravenously. Control *Acox1*^{-/-} mice were intravenously administered the Ad/LacZ construct, which harbors the β -galactosidase gene. **(a)** Low magnification, histological appearance of the liver (hematoxylin and eosin-stained sections). Hepatic parenchymal cells of *Acox1*-deficient mice show severe steatosis involving the entire liver lobule (*-/-*, inset) compared with wild type (Wt). Five days after infection with Ad/LacZ to control the efficiency of liver infection, the histological aspect of the *Acox1*^{-/-} liver is similar to that of the noninjected *Acox1*^{-/-} control mice (*-/-* and *-/-*Lz). **(b)** Livers were immunostained for ACOX1 localization 5 days after injection. Intense cytoplasmic granular staining for ACOX1 is seen in the liver of Wt mice. No expression of ACOX1 protein was detected in the *Acox1*-deficient mice (*-/-*) and in the Ad/LacZ *Acox1*^{-/-} mice (*-/-*Lz). As expected, 60–70% of hepatocytes stained positively for β -galactosidase after Ad/LacZ injection (*-/-*Lz inset). Livers *Acox1*^{-/-} infected with Ad/hACOX1a (*-/-*1a) or with Ad/hACOX1b (*-/-*1b) show respectively an homogenous (*-/-*1a, inset) or a heterogeneous expression of ACOX1 (*-/-*1b, inset). Coinfection of the *Acox1*^{-/-} liver with the both adenovirus, Ad/hACOX1a and Ad/hACOX1b, also shows a heterogeneous expression (*-/-*1ab, inset).

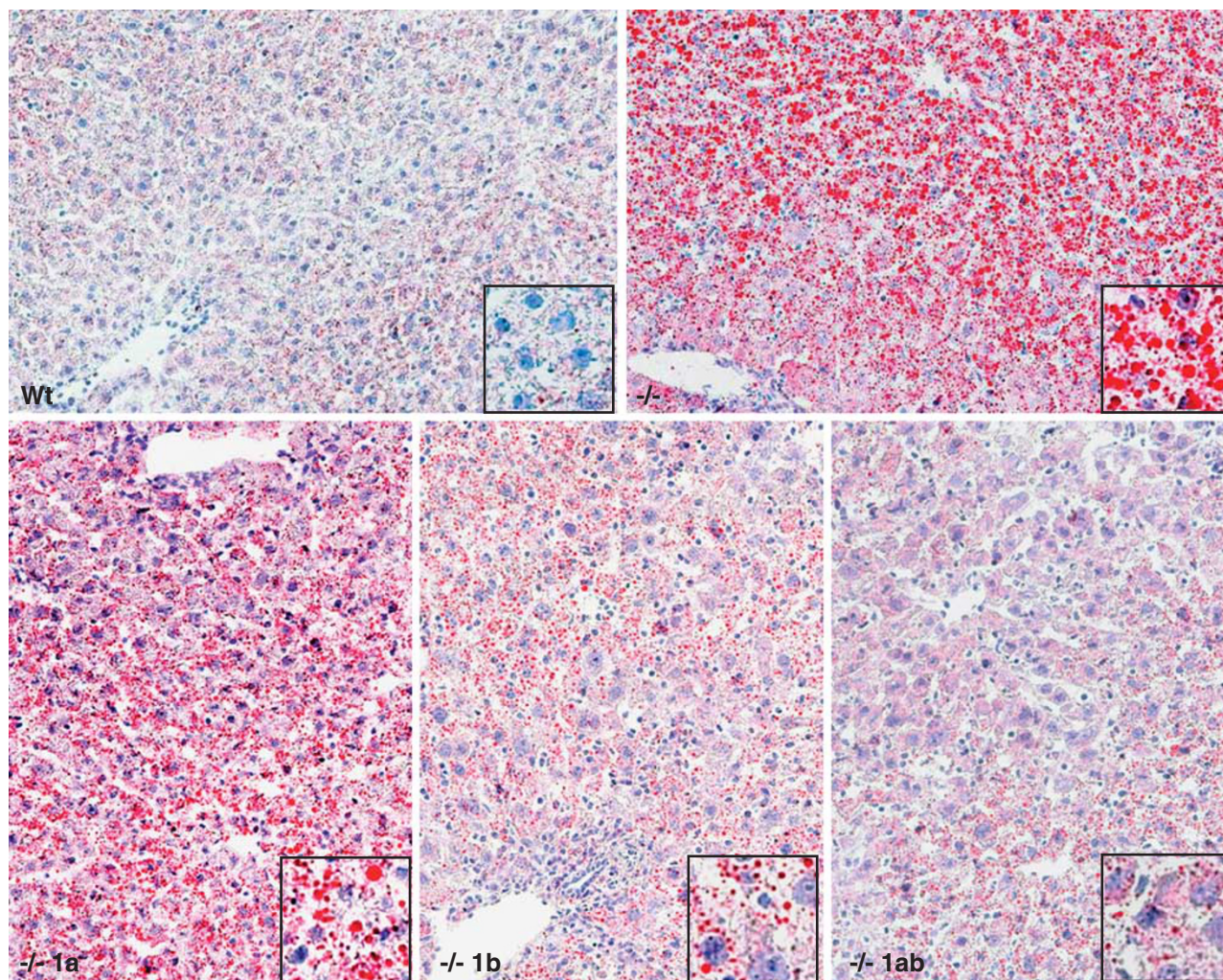


Figure 2 Hepatic lipids storage. Oil-red O-staining of liver frozen sections from wild-type (+/+) mice (Wt, inset), 2-month-old *Acox1*^{-/-} mice, which develop a hepatic steatosis (-/-, inset), Ad/hACO1a infected (-/-1a, inset), Ad/hACO1b infected (-/-1b, inset) and Ad/hACO1a/1b coinfecting (-/-1ab, inset). The neutral lipids are dyed by oil-red O-staining, which demonstrates fatty changes at 5 days in *Acox1*^{-/-} mice infected with Ad/hACO1a (-/-1a, inset) or/ and Ad/hACO1b (-/-1b, -/-1ab, insets) compared with control *Acox1* null mice (-/-, inset).

displayed a remarkable peroxisome proliferation with rare fatty hepatocytes with microvesicular lipid droplets (Figure 3 and -/-1b inset). Expression of both the ACOX1a and the ACOX1b isoforms in the mouse *Acox1*^{-/-} liver was associated with an intermediary profile including many fatty hepatocytes with a strongly reduced number of lipid vesicles and some regenerative hepatocytes with numerous peroxisomes (Figure 3 and -/-1ab inset).

Liver Cell Proliferation in ACOX1(-/-) Null Mice

A strong nuclear BrdUrd staining of hepatocytes was found in *Acox1*^{-/-} livers due to increased hepatocellular regeneration (Figure 4a, upper right, and b). Five days after injection of Ad/ACO1a or Ad/ACO1b into ACOX1 null mice, we noted a significant reduction in the number of labeled hepatocyte nuclei (Figure 4a, -/-1a, -/-1b, and b). On the other hand, expression of both the ACOX1a and the ACOX1b isoforms led

to an increase in stained nuclei of both hepatocytes and hepatic nonparenchymal cells (Figure 4a, -/-1ab inset, and b).

ACOX1-Dependent Regulation of PPAR α Target Genes

Real-time PCR and northern blot analysis of liver RNA showed spontaneous upregulation of PPAR α target gene expression in the *Acox1*^{-/-} liver (Figure 5a and b). As expected, mRNA levels of known PPAR α -regulated genes responsible for peroxisomal (L-PBE, PTL), microsomal (CYP4A10, CYP4A14) or mitochondrial (CPT1a and MCAD) fatty acid oxidation were elevated in the *Acox1*^{-/-} liver due to the spontaneous activation of PPAR α by unmetabolized endogenous ligands (Figure 5a and b). Adenofection with the ACOX1a isoform resulted in a modest reduction in the levels of these mRNAs, whereas ACOX1b had a more profound effect in reversing the increases. Administration of both isoforms together seemed to be more

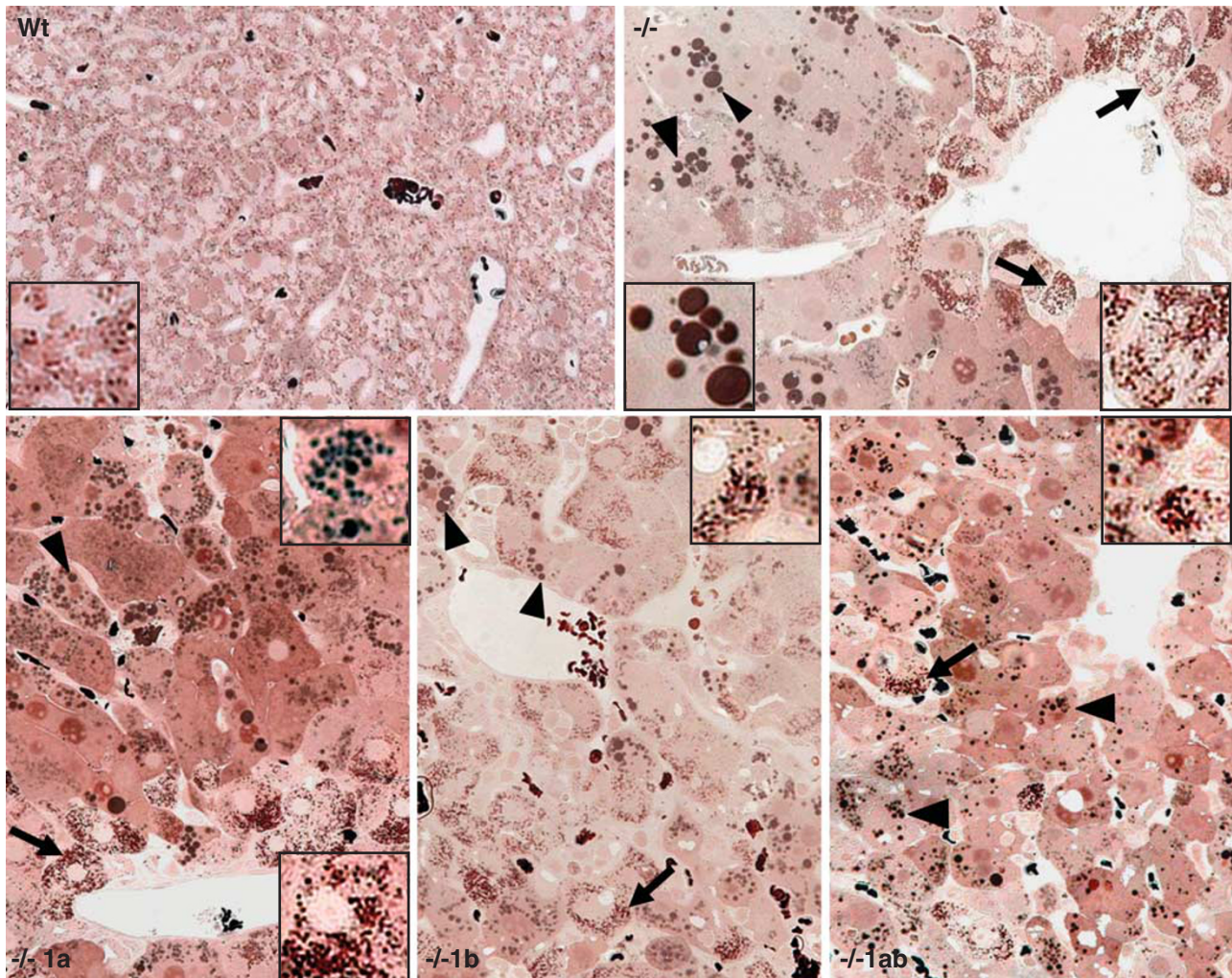


Figure 3 Spontaneous hepatic peroxisome proliferation. Light microscopic appearance of the liver as shown in semithin sections of a tissue that was processed for the cytochemical localization of catalase, due to its peroxidasic activity, using the alkaline 3',3'-diaminobenzidine substrate. *Wild-type (+/+)* mice show peroxisomes randomly distributed in the hepatocyte cytoplasm, as dark brown dots indicating the presence of diaminobenzidine reaction product (inset); Peroxisomal mosaicism, peroxisomal paucity and spontaneous peroxisome proliferation in the liver of *Acox1* null control mice (*Wt*) showing microvesicular steatosis and regenerated hepatocytes with massive peroxisome proliferation (*-/-*, insets); the hACOX1a-infected liver shows reduced lipid droplets size at 5 days (*-/-* 1a, upper inset) and peroxisome proliferation (*-/-* 1a, lower inset); hACOX1b-infected liver (*-/-* 1b); hACOX1a/1b-infected liver (*-/-* 1ab). Fat droplets of different sizes are seen in the hepatocyte cytoplasm (arrowheads). A marked spontaneous proliferation of peroxisomes occurs in numerous hepatocytes that are resistant to fatty change (arrows), as evidenced by numerous brown-stained granules. *-/-*, *-/-* 1a and *-/-* 1ab sections show no catalase containing brown dots (peroxisomes) in a majority of hepatocytes except for a rare liver cell with clusters of peroxisomes appearing as brown granules (arrows). The sinusoidal erythrocytes are stained positively (dark brown color) because of the peroxidasic activity of hemoglobin.

effective. Fatty acid transporter/CD36 mRNA content was also elevated in the *Acox1(-/-)* liver and the adenofected ACOX1 isoforms reversed this effect (Figure 5a). The amount of the three PPAR isotypes, α , β/δ and γ , was increased in the *Acox1(-/-)* null mouse liver (Figure 5a). Expression of the ACOX1a and ACOX1b isoforms in the livers obtained from the *Acox1(-/-)* mouse showed a significant decrease in mRNA levels of the PPAR α and its target genes, as well as in mRNA levels of PPAR β/δ and PPAR γ (Figure 5a).

Immunoblot analysis confirmed an increase in the content of L-PBE and PTL in the *Acox1(-/-)* mouse liver (Figure 5c). Both the expression of ACOX1b alone or ACOX1a plus ACOX1b, showed a quasi-normal expression of

both peroxisomal L-PBE and PTL proteins. To a lesser extent, the expression of ACOX1a alone also had a significant effect (Figure 5c). The immunoblot results have been confirmed by the ectopic adenofection of isolated *Acox1(-/-)* hepatocytes as shown in Figure 5c.

Recruitment of PPAR α , RXR α and Coactivators SRC-1 and PBP to L-PBE Promoter

Transcriptional activation of a target gene by PPAR α requires, in addition to heterodimerization with RXR α , recruitment of coactivators. CHIP analysis was used to examine whether recruitments of PPAR α , RXR α and coactivators (SRC-1 and PBP/Med1) to the L-PBE gene promoter were influenced

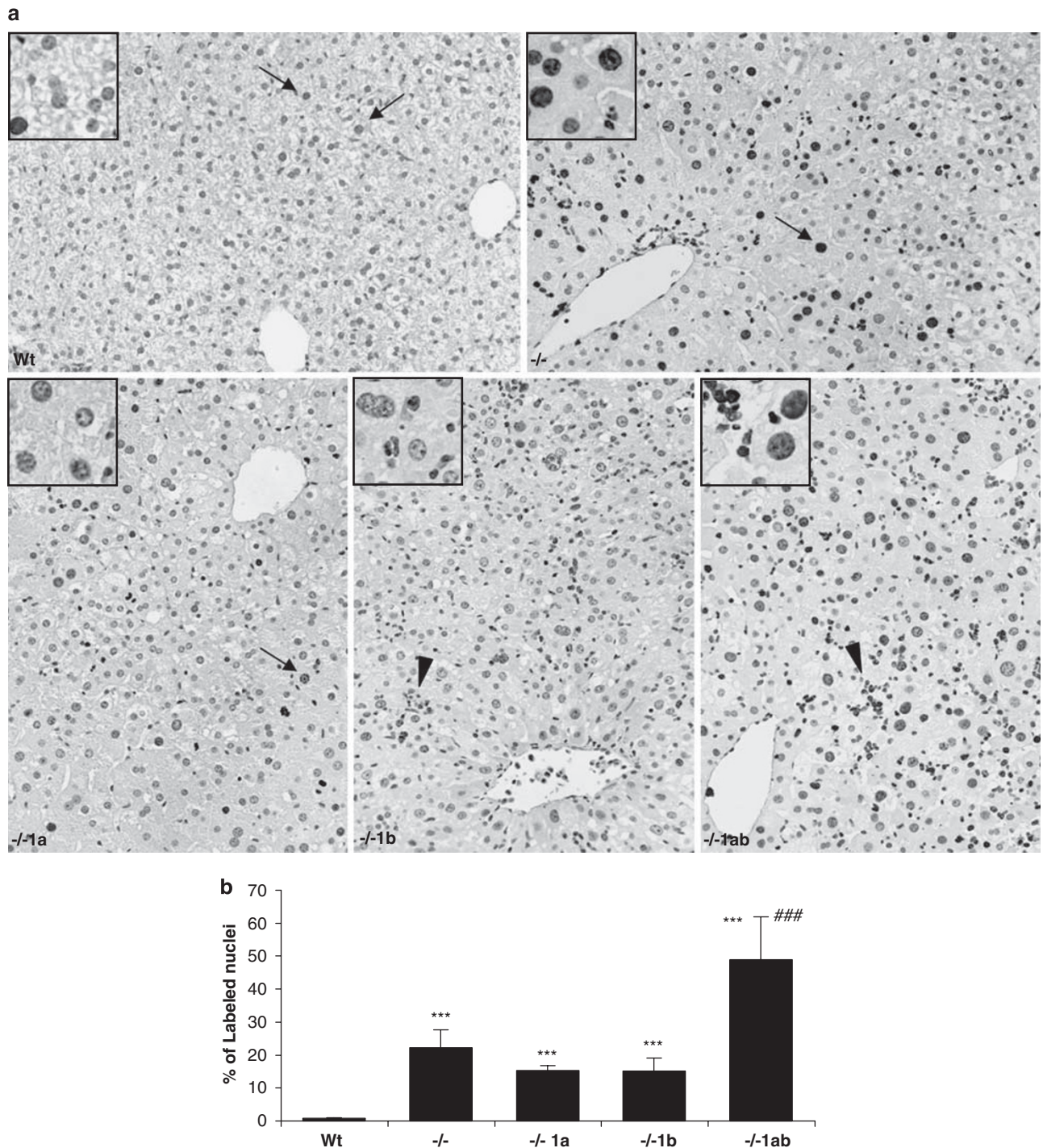


Figure 4 (a) Liver cell proliferation as assessed by bromodeoxyuridine (BrdUrd) immunohistochemical staining. (a) Hepatocytes proliferation was assessed by BrdUrd incorporation into the nuclei. Mice were administered with BrdUrd for 3 days before killing. In the wild-type (Wt) mice liver (+/+), BrdUrd labeling is confined to an occasional liver cell (Wt, arrows), whereas in *Acox1*(-/-), many cell nuclei show intense labeling indicating cell proliferation. Expression of the hACOX1a isoform (-/-1a and insert) in the *Acox1*(-/-) mice liver reduces the number of stained nuclei. The expression of hACOX1b isoform (-/-1b and insert) or both isoforms (-/-1ab and insert) in the *Acox1*(-/-) mice liver, shows an increased labeling of nonparenchymal cells (arrowheads). (b) Liver cell proliferation as assessed by BrdUrd labeling indices calculated as the percentage of labeled nuclei of Wt (+/+) mice (Wt), 2-month-old *Acox1*(-/-) mice noninfected (-/-), hACOX1a infected (-/-1a), hACOX1b infected (-/-1b), hACOX1a/1b infected (-/-1ab). All values are means \pm s.e.m. ($n=5$ per group) and are normalized to Wt. Symbols (* and #) correspond to a statistical significance of higher mean signal intensity, ($P<0.01$ for *** and ###), compared with the Wt (*) or with the *Acox1*(-/-) (#).

by the hepatic expression of the ACOX1 isoforms in *Acox1* null mice.

Livers from *Acox1*($-/-$) mice, as control, or *Acox1*($-/-$) mice expressing LacZ/adenovirus, ACOX1a, ACOX1b or both isoforms 1a and 1b of ACOX1 were used to prepare cross-linked protein-DNA extracts. The latter were immunoprecipitated with antibodies against PPAR α , RXR α , PBP/Med1 and SRC-1 (Figure 6a). DNA fragments extracted from these immunoprecipitates were analyzed by PCR using primers to amplify the PPRE of the mouse L-PBE gene. These results show that infection with mock LacZ/adenovirus has no effect on the PPAR α /RXR α -PBP/Med1-SRC1 complex recruitment (Figure 6a, lines 1 and 2). Hepatic expression of ACOX1a or ACOX1b exhibited a similar level of PPAR α /RXR α recruitment (Figure 6a, lines 3 and 4). However, in the case of ACOX1b expression, there was a net downrecruitment of SRC1 and PBP/Med1 to the L-PBE promoter (Figure 6a, line 4). This is in accordance with the downregulated level of L-PBE mRNA (Figure 5a and b). The expression of both ACOX1 isoforms 1a and 1b showed a unique profile of the L-PBE PPAR-response element in which the recruitments of PBP/Med1 and of SRC-1 were accompanied by an increased recruitment of RXR α and a net decrease in PPAR α recruitment (Figure 6a, line 5).

Thus, the expression of each ACOX1 isoform or both together resulted in the recruitment of a specific transcriptional complex, including PPAR α and/or RXR α and coactivators, suggesting that fatty acids metabolized by ACOX1 are key ligands for PPAR α or for RXR α under *in vivo* conditions.

Serum Levels of Fatty Acids

The decreased fatty acid levels of ω -3 (-79%) and ω -6 (-36%) series as measured in *Acox1*($-/-$) mice were reversed significantly by the expression of ACOX1b alone (-54% for ω -3 and -11% for ω -6) or in association with ACOX1a (-61% for ω -3 and -25% for ω -6) (Supplementary Figure S6A). Polyunsaturated fatty acids, such as arachidonic acid (AA, 20:4 ω -6) and docosahexaenoic acid (DHA, 22:6 ω -3), are known substrates (or products) of peroxisomal fatty acids oxidation¹⁶ and function as natural ligands for PPAR α .¹²⁻¹⁵ Plasma levels of these polyunsaturated fatty acids appear to be linked to the expression level of hepatic ACOX1 isoforms. Indeed, in the absence of *Acox1* a remarkable decrease in the serum levels of AA (20:4) and DHA (22:6) was found (Figure 6b and c). The expression of ACOX1a isoform alone had no effect on the levels of 20:4 and 22:6, whereas ACOX1b isoform significantly increase the level of 22:6 (Figure 6b and c). Interestingly, the expression of both ACOX1 isoforms exhibited significant increases in 20:4 and 22:6 levels (Figure 6b and c). Among different VLCFAs, the monounsaturated nervonic acid (24:1) level increased strongly upon ACOX1b expression (Figure 6d). In addition, plasma levels of other saturated and monounsaturated fatty acids from 16:0 to 24:0 carbons did not show any significant

correlation with the expression of the ACOX1 isoforms (Supplementary Figure S7).

Negative Regulation of Peroxisomal β -Oxidation Genes by DHA

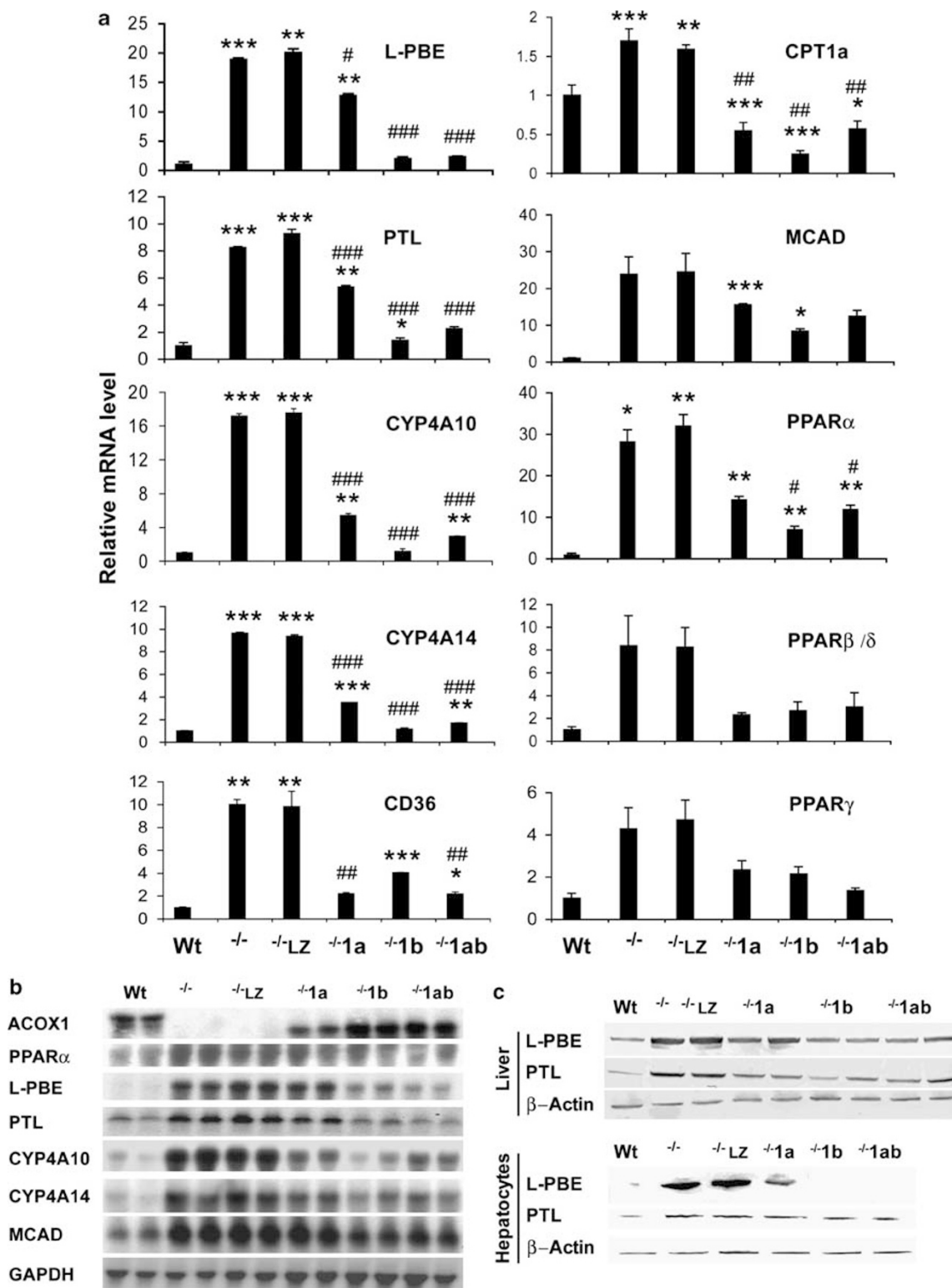
Ligand-dependent regulations of PPAR α and RXR α signaling have been tested using primary *Acox1*($-/-$) hepatocytes. When exposed to DHA, *Acox1*($-/-$) hepatocytes show a dramatic and a specific downregulation of L-PBE and PTL mRNAs in a dose-dependent manner (Figure 7a), and the western blot analysis also shows a decrease in L-PBE protein level (Figure 7b). Only 50 μ M of DHA has a significant effect on CYP4A14 mRNA level (Figure 7a). Thus, increasing the DHA level in *Acox1*($-/-$) hepatocytes, in which PPAR α target genes are overexpressed, would lead to the specific activation of RXR α and recruitment of coactivators to the peroxisomal gene promoter (Figure 6a) leading to the negative regulation of the corresponding genes. This shows a feedback loop between the expression of peroxisomal β -oxidation genes involved in DHA synthesis and DHA-dependent activation of RXR α . On the other hand, treatment of *Acox1*($-/-$) hepatocytes with nervonic acid (24:1) shows no significant effect on the mRNA levels of genes involved in the peroxisomal β -oxidation or microsomal ω -oxidation pathways (Figure 7a). However, western blot analysis shows that L-PBE protein level is slightly decreased by 24:1 treatment showing a possible posttranslational regulation by nervonic acid.

DISCUSSION

Fatty acids are metabolized in the liver by two distinct β -oxidation systems localized in the mitochondria and peroxisomes.^{3,13,16} The β -oxidation of medium and LCFAs occurs mainly in the mitochondria, whereas that of VLCFAs takes place exclusively in peroxisomes.^{13,16} In addition, the microsomal ω -oxidation system, which includes the CYP4A10 and CYP4A14 enzymes, participates in the transformation of LCFAs and VLCFAs into DCAs, which are further β -oxidized in peroxisomes.^{16,17} The mitochondria metabolize the bulk of dietary fatty acids for energetic purposes, whereas the extramitochondrial fatty acid oxidation systems in peroxisomes and endoplasmic reticulum only have a minor role in this respect.^{3,13,16} Accordingly, mice treated with tetradecylglycidic acid, an irreversible inhibitor of CPT1, a key enzyme in the control of mitochondrial β -oxidation, develop massive microvesicular hepatic steatosis.²⁴ The mitochondrial fatty acid β -oxidation enzyme system abnormalities lead to disturbances in hepatic lipid metabolism with accumulation of lipid in hepatocytes.^{25,26} It is also evident that the disruption of the peroxisomal *Acox1* gene in the mouse affects hepatic lipid metabolism and contributes to the development of severe microvesicular hepatic steatosis.^{1,3} The sustained activation of PPAR α and the upregulation of PPAR α target genes contribute to the hepatocellular regeneration with evidence of a spontaneous massive peroxisome proliferation leading to hepatocellular carcinomas.^{1,2}

In this study, we found that hepatic steatosis that develops in mice lacking *Acox1* is attenuated upon expression of the human ACOX1b isoform and completely reversed upon expression of both the human ACOX1 isoforms 1a and 1b

(Figure 1). The weaker reversal of the *Acox1*^{-/-} phenotype by ACOX1a expression can be attributed at least in part to the weaker expression of ACOX1a after adenofection. Nevertheless, previous data from recombinant human



ACOX1a characterization²¹ or expression in the *fox1Δ* deletion mutant of *Saccharomyces cerevisiae*²² have shown that ACOX1a is more labile and exhibits reduced activity

toward palmitoyl-CoA as compared with ACOX1b. It is likely that ACOX1a functions as a heterodimer with ACOX1b, explaining conclusively why the expression of ACOX1a

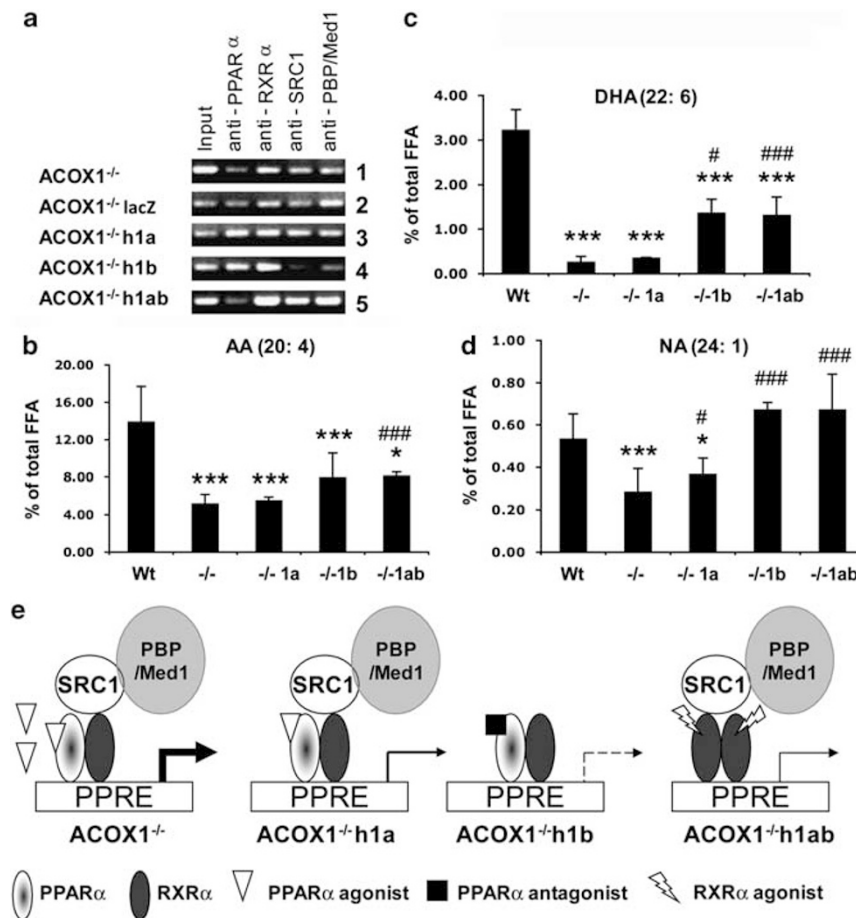


Figure 6 (a) Differential recruitment of PPAR α and its coactivators to L-PBE gene promoter. Chromatin immunoprecipitation assays were performed with specific antibodies to show recruitment of PPAR α and coactivators to the L-PBE-response unit in *Acox1*^{-/-} mice liver noninfected (lane 1) or Ad/LacZ infected (lane 2) as control or *Acox1*^{-/-} mice infected with ACOX1a (*Acox1*^{-/-} 1a, lane 3), ACOX1b (*Acox1*^{-/-} 1b, lane 4) or ACOX1a and ACOX1b (*Acox1*^{-/-} 1ab, lane 5). Antibodies used for ChIP assays: peroxisome anti-PPAR α , RXR α , anti-RXR α (9-cis retinoic acid X receptor- α); anti-PBP/Med1 (PBP/Med1, peroxisome proliferator-activated receptor-interacting protein/Mediator 1) and anti-SRC1 (SRC-1, steroid receptor coactivator-1) (see the Supplementary Materials and Methods section). (b–d) Plasmatic levels of polyunsaturated fatty acids of wild-type mice (Wt), 2-month-old *Acox1*^{-/-} (–/–), Ad/hACOX1a infected (–/–1a), Ad/hACOX1b infected (–/–1b) and Ad/hACOX1a/1b coinfected (–/–1ab). AA (22:4): arachidonic acid, DHA (22:6): docosahexanoic acid, NA (24:1): nervonic acid. Values represent means \pm s.e.m. ($n=4-5$ per group) and are normalized to total fatty acids in the Wt. Symbols (* and #) correspond to a statistical significance of higher mean signal intensity, ($P<0.001$ for *** and ### $P<0.01$ for ** and ## $P<0.05$ for * and #), compared with the Wt (*) or with the *Acox1*^{-/-} (#). (e) Schematic of PPAR α , RXR α and coactivators (PBP/Med1 and SRC-1) recruitments to PPAR α target genes PPRE in the mouse livers of *Acox1*^{-/-}, *Acox1*^{-/-} 1a, *Acox1*^{-/-} 1b or *Acox1*^{-/-} 1ab.

Figure 5 Hepatic ACOX1 expression effect on the regulation of PPARs and their target genes. (a) Real-time PCR was used to quantify the hepatic mRNA levels at 5 days after infection of PPAR α and its target genes: L-PBE, PTL, CYP4A10, CYP4A14, CD36, CPT1a and MCAD. The mRNA levels of PPAR β/δ and PPAR γ were also determined in wild-type mice (Wt), 2-month-old *Acox1*^{-/-} mice, Ad/LacZ infected (–/–LZ), Ad/hACOX1a infected (–/–1a), Ad/hACOX1b infected (–/–1b) and Ad/hACOX1a/1b coinfected (–/–1ab). All real-time PCR reactions were performed in duplicate (used primers are presented in the Supplementary Table S1). All values are means \pm s.e.m. ($n=5$ per group) and are normalized to wild type. Symbols (* and #) correspond to a statistical significance of higher mean signal intensity, ($P<0.01$ for *** and ### $P<0.02$ for ** and ## $P<0.05$ for * and #), compared with the wild type (*) or with the *Acox1*^{-/-} (#). (b) Northern blot analysis of hepatic PPAR α and its targets genes. (c) Western blots to assess the expression of peroxisomal PPAR α -target genes in wild-type mice (Wt), 2-month-old *Acox1*^{-/-} mice, Ad/LacZ infected (–/–LZ), Ad/hACOX1a infected (–/–1a), Ad/hACOX1b infected (–/–1b) and Ad/hACOX1a/1b coinfected (–/–1ab). Western blots were performed in both liver tissues from infected mice or from ectopically infected hepatocytes isolated as described in the Supplementary Materials and Methods section.

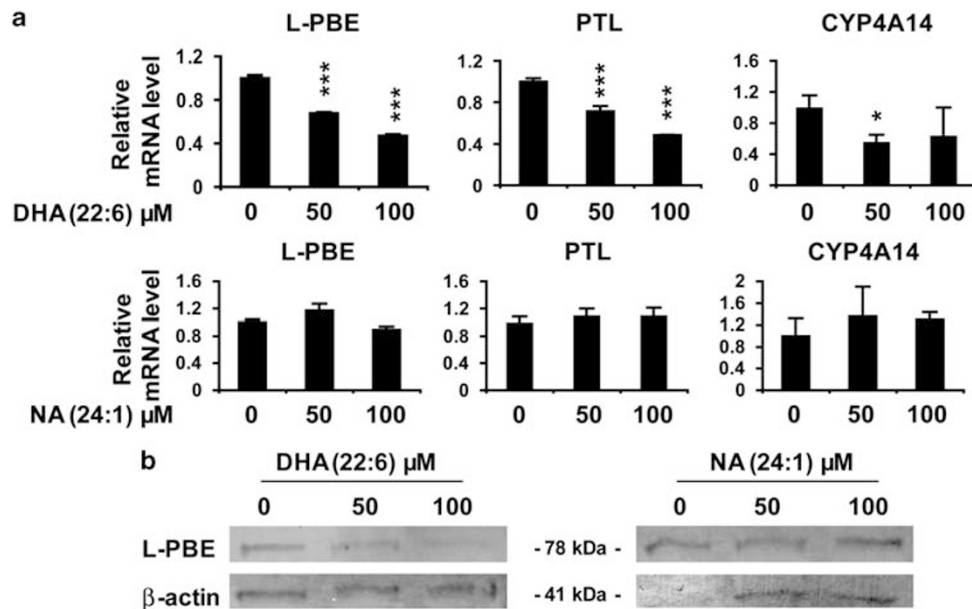


Figure 7 Specific peroxisomal gene regulation by DHA and nervonic acid in *Acox1*^{-/-} hepatocytes. Isolated *Acox1*^{-/-} hepatocytes were treated with DHA or nervonic acid at indicated concentrations during 48 h. Control *Acox1*^{-/-} hepatocytes were treated with dimethylsulfoxide as vehicle. (a) Real-time PCR was used to quantitate the mRNA levels of PPAR α target genes: L-PBE, PTL and CYP4A14. All real-time PCR reactions were performed in duplicate. Values represent means \pm s.e.m. ($n = 3$ per group) and are normalized to wild type. Symbol (*) correspond to a statistical significance of higher mean signal intensity, ($P < 0.01$ for ***, $P < 0.05$ for *), compared with the control-untreated *Acox1*^{-/-} hepatocytes. (b) Western blots were performed using cell extracts from *Acox1*^{-/-} hepatocytes treated as indicated above with anti-LPBE or anti-actin as described in the Supplementary Material and Methods section.

isoform with ACOX1b is more effective in the reversal of *Acox1*^{-/-} phenotype. In these mice, several upregulated PPAR α target genes coding for hepatic mitochondrial (MCAD, CPT-1a), microsomal (CYP4A10 and CYP4A14) and peroxisomal (L-PBE, PTL) proteins^{6,13} were downregulated following the expression of human ACOX1 isoforms. This implies that the sustained hyperactivation of PPAR α as caused by substrates which are left unmetabolized in the absence of ACOX1 and that function as PPAR α ligands, are degraded upon expression of the human ACOX1 isoforms in the *Acox1*^{-/-} mouse. In ACOX1 null mice, the accumulation in the liver of ACOX1 substrates, such as LCFAs, VLCFAs or their acyl-CoAs, triggered the spontaneous sustained PPAR α hyperactivity analogous to that seen in the livers of wild-type mice exposed to synthetic peroxisome proliferators.¹³ In these mice, absence of peroxisomal fatty acid oxidation and induction of fatty acid ω -oxidation was found to lead to increased levels of DCAs that are toxic to the mitochondria, as they can uncouple oxidative phosphorylation.²⁷ The expression of ACOX1b, or both ACOX1 isoforms reversed this process probably by degrading these natural PPAR α ligands, thereby attenuating the sustained PPAR α sensing. Reduced PPAR α activation leads to a decrease in the generation of toxic DCAs by the extramitochondrial fatty acid oxidation pathway and minimizes mitochondrial damage leading to a reduction in hepatic steatosis. Support for the role of DCAs and PPAR α hyperactivation is also derived from the observation that *Acox1* and *Ppar α* double

nullizygous mice do not exhibit hepatic steatosis, implying that failure to induce CYP4A enzymes abrogates the production of these toxic derivatives.^{3,13} This underscores the fact that hepatic steatosis developed in *Acox1* null mice is strictly PPAR α dependent. Treatment of *Acox1*^{-/-} mice with synthetic peroxisome proliferators did not result in an additive induction of PPAR α target genes, which suggests that natural ligands saturate PPAR α in the *Acox1*^{-/-} liver.^{3,13} In these livers, analysis of PPAR γ and PPAR δ/β mRNAs levels showed no significant variations.

Analysis of circulating levels of unsaturated VLCFAs, regarded as PPAR α agonists *in vitro*, showed that the expression of human ACOX1b alone, or in combination with ACOX1a, is accompanied by a significant increase in the level of nervonic acid (24:1), which is generated from the peroxisomal β -oxidation shortening of 26:1-CoA.^{16,28} Recent data have shown that the CoA ester of nervonic acid (nervonyl-CoA) binds with high affinity to PPAR α leading to a reduction in the recruitment of coactivators, such as CBP (cAMP response element-binding protein-binding protein).²⁹ In addition, nervonic acid exerts a negative effect on the peroxisomal oxidation system³⁰ and fails to activate PPAR α .³¹ Hence, our findings point to the existence of an enzyme/product negative feedback mechanism in which nervonyl-CoA as produced by ACOX1b, a likely antagonist of PPAR α . This may explain, why after expression of human ACOX1b, a reduction was found in the recruitment of PBP/Med1 and SRC-1 coactivators to response elements of PPAR α target genes and their subsequent

downregulation. Furthermore, recent data have shown that the monounsaturated fatty acid, C16:1n7-palmitoleate derived from *de novo* synthesis, decreases activation of PPAR α target gene and suppresses hepatosteatosis.^{32,33}

In contrast to the expression of ACOX1b and increasing level of nervonic acid, the expression of both ACOX1 isoforms is accompanied by increased AA (20:4) and DHA (22:6) levels in serum of *Acox1(-/-)* mice. Interestingly, synthesis of DHA from its precursor tetracosahexanoic acid (24:6) is fully dependent on the functional peroxisomal β -oxidation pathway in both mouse and humans.¹⁶ Accordingly, the ChIP assay showed a unique profile of the L-PBE PPAR α -response unit for which the recruitments of coactivators, PBP/Med1 and of SRC-1, are accompanied by a dominant recruitment of RXR α instead of PPAR α . This is not surprising, as DHA activates RXR α in the adult mouse brain and promotes interaction between RXR α and SRC-1.³⁴ Accordingly, the RXR α homodimer signaling pathway by PPAR-response units is fully functional and can rescue the severe hypothermia phenotype observed in fasted *Ppar α -/-* mice.³⁵ Thus, ACOX1 isoforms produce the endogenous ligand of RXR α , the n-3 polyunsaturated DHA (22:6), which activates RXR α and the recruitment of coactivators (Figure 6e). As a universal hepatic integrator, RXR α heterodimerizes with several nuclear receptors, such as FXR, LXR, PPAR and TR, and thereby controls several metabolic pathways, including liver lipid metabolism.³⁶ Interestingly, supplying *Acox1(-/-)* hepatocytes with DHA leads to a downregulation of peroxisomal β -oxidation pathway (Figure 7). This points to an original cross talk between RXR α and ACOX1, the former assuring the basal expression of ACOX1 activity and the latter taking care of the production of DHA, as a natural ligand of RXR α .

In summary, the observations described in this study clearly show that the human ACOX1b isoform reverses the *Acox1* null mice fatty liver phenotype by reducing PPAR α activation and its subsequent effects on fatty acids metabolism. Our data also point to a unique cross talk between the ACOX1 isoform and both PPAR α and RXR α activations, thus implying a unique role of each of the two ACOX1 isoforms in controlling the intracellular levels of the endogenous ligands of PPAR α and RXR α , respectively. Our data suggest that it may well be important to assess the relative levels of PPAR α , RXR α and the ACOX1 isoforms in human nonalcoholic fatty liver disease, which is recognized as a leading cause of liver damage and cirrhosis in developed countries.

Supplementary Information accompanies the paper on the Laboratory Investigation website (<http://www.laboratoryinvestigation.org>)

ACKNOWLEDGEMENT

Financial support for this study was received from a grant from the European Union project 'Peroxisome' LSHG-CT 2004-512018, The Institut National de la Santé et de la Recherche Médicale, the Regional Council of Burgundy, the Ministère de l'enseignement Supérieur et de la Recherche and from the National Institut of Health GM 23750.

DISCLOSURE/CONFLICT OF INTEREST

The authors declare no conflict of interest.

1. Fan CY, Pan J, Chu R, *et al*. Hepatocellular and hepatic peroxisomal alterations in mice with a disrupted peroxisomal fatty acyl-coenzyme A oxidase gene. *J Biol Chem* 1996;271:24698-24710.
2. Fan CY, Pan J, Usuda N, *et al*. Steatohepatitis, spontaneous peroxisome proliferation and liver tumors in mice lacking peroxisomal fatty acyl-CoA oxidase. Implications for peroxisome proliferator-activated receptor alpha natural ligand metabolism. *J Biol Chem* 1998;273:15639-15645.
3. Hashimoto T, Fujita T, Usuda N, *et al*. Peroxisomal and mitochondrial fatty acid beta-oxidation in mice nullizygous for both peroxisome proliferator-activated receptor alpha and peroxisomal fatty acyl-CoA oxidase. Genotype correlation with fatty liver phenotype. *J Biol Chem* 1999;274:19228-19236.
4. Yeldandi AV, Rao MS, Reddy JK. Hydrogen peroxide generation in peroxisome proliferator-induced oncogenesis. *Mutat Res* 2000;448:159-177.
5. Issemann I, Green S. Activation of a member of the steroid hormone receptor superfamily by peroxisome proliferators. *Nature* 1990;347:645-650.
6. Kliewer SA, Umehara K, Noonan DJ, *et al*. Convergence of 9-cis retinoic acid and peroxisome proliferator signalling pathways through heterodimer formation of their receptors. *Nature* 1992;358:771-774.
7. Cherkaoui-Malki M, Meyer K, Cao WQ, *et al*. Identification of novel peroxisome proliferator-activated receptor alpha (PPARalpha) target genes in mouse liver using cDNA microarray analysis. *Gene Expr* 2001;9:291-304.
8. Lemberger T, Desvergne B, Wahli W. Peroxisome proliferator-activated receptors: a nuclear receptor signaling pathway in lipid physiology. *Annu Rev Cell Dev Biol* 1996;12:335-363.
9. Jia Y, Qi C, Kashireddi P, *et al*. Transcription coactivator PBP, the peroxisome proliferator-activated receptor (PPAR)-binding protein, is required for PPARalpha-regulated gene expression in liver. *J Biol Chem* 2004;279:24427-24434.
10. Yuan CX, Ito M, Fondell JD, *et al*. The TRAP220 component of a thyroid hormone receptor-associated protein (TRAP) coactivator complex interacts directly with nuclear receptors in a ligand-dependent fashion. *Proc Natl Acad Sci USA* 1998;95:7939-7944.
11. Rachez C, Lemon BD, Suldan Z, *et al*. Ligand-dependent transcription activation by nuclear receptors requires the DRIP complex. *Nature* 1999;398:824-828.
12. Lee SS, Pineau T, Drago J, *et al*. Targeted disruption of the alpha isoform of the peroxisome proliferator-activated receptor gene in mice results in abolishment of the pleiotropic effects of peroxisome proliferators. *Mol Cell Biol* 1995;15:3012-3022.
13. Reddy JK. Peroxisome proliferators and peroxisome proliferator-activated receptor alpha: biotic and xenobiotic sensing. *Am J Pathol* 2004;164:2305-2321.
14. Gottlicher M, Widmark E, Li Q, *et al*. Fatty acids activate a chimera of the clofibrate acid-activated receptor and the glucocorticoid receptor. *Proc Natl Acad Sci USA* 1992;89:4653-4657.
15. Forman BM, Chen J, Evans RM. Hypolipidemic drugs, polyunsaturated fatty acids, and eicosanoids are ligands for peroxisome proliferator-activated receptors alpha and delta. *Proc Natl Acad Sci USA* 1997;94:4312-4317.
16. Wanders RJ. Peroxisomes, lipid metabolism, and peroxisomal disorders. *Mol Genet Metab* 2004;83:16-27.
17. Aoyama T, Hardwick JP, Imaoka S, *et al*. Clofibrate-inducible rat hepatic P450s IVA1 and IVA3 catalyze the omega- and (omega-1)-hydroxylation of fatty acids and the omega-hydroxylation of prostaglandins E1 and F2 alpha. *J Lipid Res* 1990;31:1477-1482.
18. Fournier B, Saudubray JM, Benichou B, *et al*. Large deletion of the peroxisomal acyl-CoA oxidase gene in pseudoneonatal adrenoleukodystrophy. *J Clin Invest* 1994;94:526-531.
19. Varanasi U, Chu R, Chu S, *et al*. Isolation of the human peroxisomal acyl-CoA oxidase gene: organization, promoter analysis, and chromosomal localization. *Proc Natl Acad Sci USA* 1994;91:3107-3111.

20. Morais S, Knoll-Gellida A, Andre M, *et al*. Conserved expression of alternative splicing variants of peroxisomal acyl-CoA oxidase 1 in vertebrates and developmental and nutritional regulation in fish. *Physiol Genomics* 2007;28:239–252.
21. Oaxaca-Castillo D, Andreoletti P, Vluggens A, *et al*. Biochemical characterization of two functional human liver acyl-CoA oxidase isoforms 1a and 1b encoded by a single gene. *Biochem Biophys Res Commun* 2007;360:314–319.
22. Ferdinandusse S, Denis S, Hogenhout EM, *et al*. Clinical, biochemical, and mutational spectrum of peroxisomal acyl-coenzyme A oxidase deficiency. *Hum Mutat* 2007;28:904–912.
23. Yu S, Cao WQ, Kashireddy P, *et al*. Human peroxisome proliferator-activated receptor alpha (PPARalpha) supports the induction of peroxisome proliferation in PPARalpha-deficient mouse liver. *J Biol Chem* 2001;276:42485–42491.
24. van der Leij FR, Bloks VW, Grefhorst A, *et al*. Gene expression profiling in livers of mice after acute inhibition of beta-oxidation. *Genomics* 2007;90:680–689.
25. Rao MS, Reddy JK. PPARalpha in the pathogenesis of fatty liver disease. *Hepatology* 2004;40:783–786.
26. Postic C, Girard J. Contribution of *de novo* fatty acid synthesis to hepatic steatosis and insulin resistance: lessons from genetically engineered mice. *J Clin Invest* 2008;118:829–838.
27. Tongsgard JH, Getz GS. Effect of Reye's syndrome serum on isolated chinchilla liver mitochondria. *J Clin Invest* 1985;76:816–825.
28. Sandhir R, Khan M, Chahal A, *et al*. Localization of nervonic acid beta-oxidation in human and rodent peroxisomes: impaired oxidation in Zellweger syndrome and X-linked adrenoleukodystrophy. *J Lipid Res* 1998;39:2161–2171.
29. Hostetler HA, Kier AB, Schroeder F. Very-long-chain and branched-chain fatty acyl-CoAs are high affinity ligands for the peroxisome proliferator-activated receptor alpha (PPARalpha). *Biochemistry* 2006;45:7669–7681.
30. Flatmark T, Christiansen EN, Kryvi H. Evidence for a negative modulating effect of erucic acid on the peroxisomal beta-oxidation enzyme system and biogenesis in rat liver. *Biochim Biophys Acta* 1983;753:460–466.
31. Krey G, Braissant O, L'Horsset F, *et al*. Fatty acids, eicosanoids, and hypolipidemic agents identified as ligands of peroxisome proliferator-activated receptors by coactivator-dependent receptor ligand assay. *Mol Endocrinol* 1997;11:779–791.
32. Cao H, Gerhold K, Mayers JR, *et al*. Identification of a lipokine, a lipid hormone linking adipose tissue to systemic metabolism. *Cell* 2008;134:933–944.
33. Olefsky JM. Fat talks, liver and muscle listen. *Cell* 2008;134:914–916.
34. de Urquiza AM, Liu S, Sjoberg M, *et al*. Docosahexaenoic acid, a ligand for the retinoid X receptor in mouse brain. *Science* 2000;290:2140–2144.
35. Ijpenberg A, Tan NS, Gelman L, *et al*. *In vivo* activation of PPAR target genes by RXR homodimers. *EMBO J* 2004;23:2083–2091.
36. Wan YJ, An D, Cai Y, *et al*. Hepatocyte-specific mutation establishes retinoid X receptor alpha as a heterodimeric integrator of multiple physiological processes in the liver. *Mol Cell Biol* 2000;20:4436–4444.